

Suppression of transport in nondisordered quantum spin chains due to confined excitationsPaolo Pietro Mazza,¹ Gabriele Peretto,¹ Alessio Lerose,¹ Mario Collura,² and Andrea Gambassi¹¹*SISSA – International School for Advanced Studies & INFN, via Bonomea 265, 34136 Trieste, Italy*²*The Rudolf Peierls Centre for Theoretical Physics, Oxford University, Oxford OX1 3NP, United Kingdom*

(Received 26 June 2018; revised manuscript received 22 January 2019; published 21 May 2019)

The laws of thermodynamics require any initial macroscopic inhomogeneity in extended many-body systems to be smoothed out by the time evolution through the activation of transport processes. In generic quantum systems, transport is expected to be governed by a diffusion law, whereas a sufficiently strong quenched disorder can suppress it completely due to many-body localization of quantum excitations. Here, we show that the confinement of quasiparticles can also suppress transport even if the dynamics are generated by nondisordered Hamiltonians. We demonstrate this in the quantum Ising chain with transverse and longitudinal magnetic fields, prepared in a paradigmatic state with a domain wall and thus with a spatially varying energy density. We perform extensive numerical simulations of the dynamics which turn out to be in excellent agreement with an effective analytical description valid within both weak and strong confinement regimes. Our results show that the energy flow from “hot” to “cold” regions of the chain is suppressed for all accessible times. We argue that this phenomenon is general, as it relies solely on the emergence of confinement of excitations.

DOI: [10.1103/PhysRevB.99.180302](https://doi.org/10.1103/PhysRevB.99.180302)

Introduction. Transport is the fundamental mechanism which allows both classical and quantum isolated and extended statistical systems to smooth out any inhomogeneity possibly present in their initial conditions, while relaxing towards their stationary states. In the quantum realm, the interest in this aspect of nonequilibrium dynamics [1–3] has been recently prompted by an impressive advance in experimental techniques with cold atoms, which made it possible to maintain coherent quantum dynamics for sufficiently long times [4–18].

Of paramount importance, in this context, is to understand whether and how the transport of conserved physical quantities, such as particle and energy densities, occurs [19,20]. Generically, the spatial spreading of local inhomogeneities is expected to obey a diffusion law, whose microscopic origin is usually traced back to inelastic collisions [21,22]. In the specific case of integrable systems, instead—characterized by an infinite set of (quasi-) local conserved quantities—transport is enhanced by the existence of stable excitations traveling ballistically with certain characteristic velocities, typically exposed after a sudden change (*quench*) in the parameters of the systems [23–27]. Correspondingly, a nonequilibrium stationary state may arise, supporting ballistic transport and thus finite currents at long times [28–38]. A completely different scenario emerges in the presence of strong disorder. In fact, in the so-called many-body localized phase [39–41], the localization of excitations [42–44] suppresses the energy and particle transport and the system fails to thermalize: Initial gradients of local quantities persist for arbitrarily long times during the evolution [45–47].

Disordered-induced localization, however, is not the sole mechanism which hampers the propagation of information in many-body interacting systems [48–51]. Indeed, even in the absence of disorder, the dynamical *confinement* of excitations [52,53] can suppress the spreading of correlations [54]. How

can this be reconciled with the heuristic expectation that an initial inhomogeneous configuration has to be smoothed out by the evolution? In this Rapid Communication we address this issue and show that a nonintegrable, nondisordered quantum spin chain with confined excitations, initially prepared in domain-wall states causing a finite energy gradient across the system, can exhibit suppression of energy transport. Although we focus here on the paradigmatic quantum Ising chain, introduced further below, the results we obtain are general and apply to a variety of physical systems since they solely rely on the confinement of the excitations, which has been shown to emerge in several other one-dimensional condensed-matter models [55–61] as well as lattice gauge theories [62–64].

Model and protocol. We consider a ferromagnetic quantum Ising chain with a transverse and a longitudinal magnetic field, h_z and h_x , respectively,

$$H(h_z, h_x) = -J \sum_{i=1}^{L-1} \sigma_i^x \sigma_{i+1}^x - h_z \sum_{i=1}^L \sigma_i^z - h_x \sum_{i=1}^L \sigma_i^x. \quad (1)$$

Here, $\sigma_i^{x,y,z}$ are the Pauli matrices acting on the site i , $J > 0$ is the Ising exchange parameter, L the (even) system size, and we consider open boundary conditions. For $h_x = 0$, the model is exactly solvable in terms of free fermions [65–67] which, in the ferromagnetic phase with $|h_z| < J$, physically correspond to freely moving domain walls (or kinks) connecting the two oppositely magnetized ground states with $\langle \sigma_j^x \rangle \neq 0$. A finite $h_x \neq 0$ causes a nonperturbative modification of the spectrum of the elementary excitations: It selects as a ground state the one with $\langle \sigma_j^x \rangle$ along h_x and raises the energy of configurations with domains of reversed spins by an amount proportional to their extension. This corresponds to a linear, V-shaped interaction potential between two consecutive kinks delimiting a domain, which therefore become *confined* into composite objects called *mesons*, in analogy with the low-energy limit of

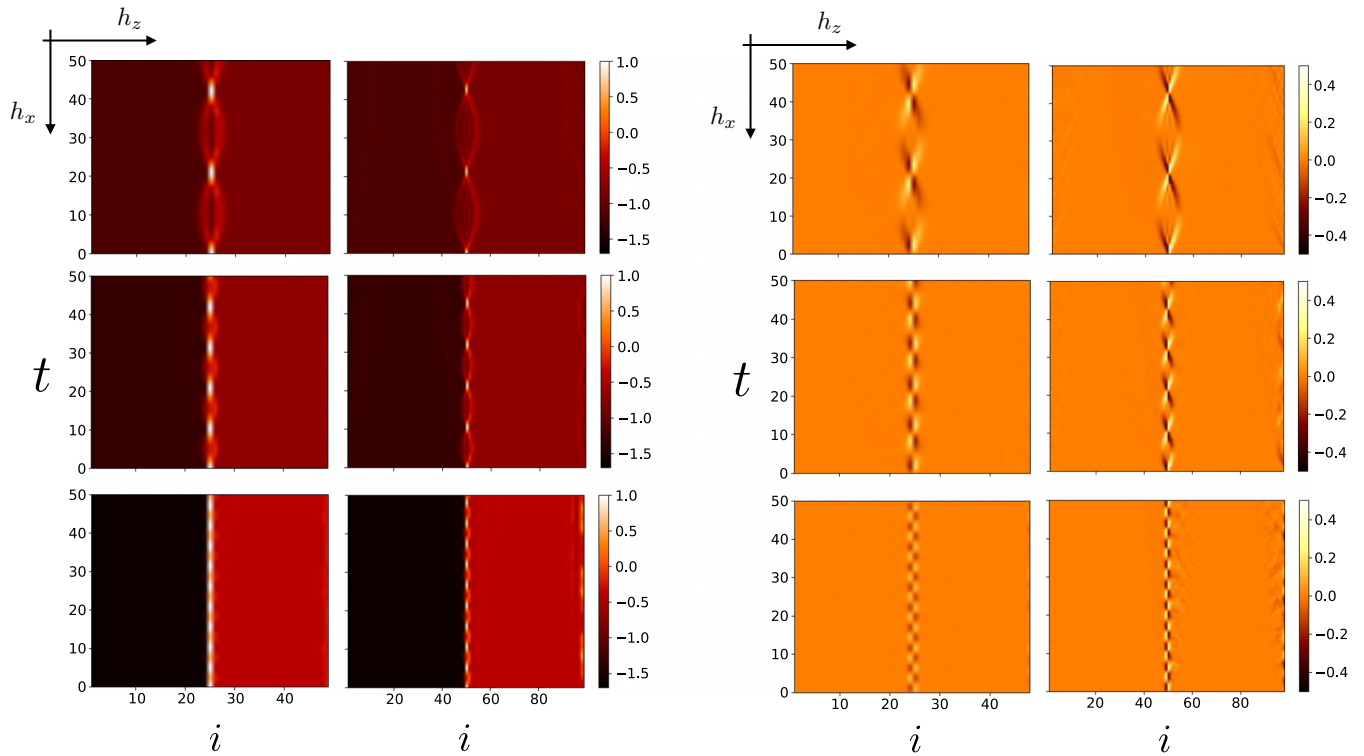


FIG. 1. Evolution of the energy density $\langle \mathcal{H}_j(t) \rangle$ (left panel) and of the energy current density $\langle \mathcal{J}_j(t) \rangle$ (right panel) profiles, governed by the Hamiltonian (1) starting from the inhomogeneous domain-wall state (2), obtained from TEBD simulations, for a range of increasing field values $h_z = 0.2$ ($L = 50$), 0.4 ($L = 100$), and $h_x = 0.15, 0.3, 0.6$, varying as indicated by the axes. (Units are fixed such that $J = 1$.) The same qualitative behavior as that illustrated here persists up to long times $t = 10^3$. Note the oscillations of the profiles around the junction, with spatial amplitude $\propto h_z/h_x$ and frequency $\propto h_x$, while there is no evidence for the activation of transport.

quantum chromodynamics. This modification of the spectrum has been studied both in the vicinity of the critical point $h_z \rightarrow 1$ exploiting field-theoretical methods [52,68,69], and far away from it in the regime of low-density excitations for small h_x [70].

In order to investigate transport processes it is convenient to consider a so-called *inhomogeneous quench* [71,72] in which two complementary subsystems are initially prepared in two different equilibrium states and then they are joined at time $t = 0$, such that they evolve according to a common, homogeneous Hamiltonian. Here, we consider a domain-wall initial state with a single kink in the middle of the chain which reads, in terms of the eigenstates $|\uparrow\rangle_j$ and $|\downarrow\rangle_j$ of σ_j^x ,

$$|\Psi_0\rangle = \bigotimes_{j=1}^{L/2} |\uparrow\rangle_j \bigotimes_{j=L/2+1}^L |\downarrow\rangle_j \equiv |\uparrow\uparrow \cdots \uparrow\uparrow\downarrow\downarrow \cdots \downarrow\downarrow\rangle, \quad (2)$$

and which is also an eigenstate of $H(0, h_x)$. At time $t > 0$, the transverse field $h_z \neq 0$ is suddenly switched on and we study the nonequilibrium evolution of the energy density profile $\langle \mathcal{H}_j(t) \rangle$ as a function of j , where

$$\mathcal{H}_j = -J\sigma_j^x\sigma_{j+1}^x - \frac{h_z}{2}(\sigma_j^z + \sigma_{j+1}^z) - \frac{h_x}{2}(\sigma_j^x + \sigma_{j+1}^x). \quad (3)$$

For $h_x = 0$, the initial energy density $\langle \mathcal{H}_j(0) \rangle$ is equal on the two sides of the junction, due to the \mathbb{Z}_2 symmetry. However, in the presence of a nonvanishing $h_x > 0$, the chain acquires an initial macroscopic energy imbalance between the left

(“cold”) part and the right (“hot”) part. In particular, the latter may be viewed as a “false vacuum” whose energy lies in the middle of the many-body spectrum, and may thereby be expected to decay into a finite density of traveling excitations upon activating the transverse field $h_z \neq 0$, leading to a meltdown of the initial imbalance after a transient [73]. In the following, we provide compelling evidence against this expectation.

Numerical analysis. In order to explore numerically the nonequilibrium evolution of the chain, we employ time-evolving block decimation (TEBD) simulations [74]. It turns out that the entanglement grows slowly up to moderate values of the field $h_z \lesssim 0.4J$, which allows us to extend the simulations to long times $t_M = 10^3 J^{-1}$ with modest computational efforts, as in the case of Ref. [54]. We investigate the behavior of $\langle \mathcal{H}_j(t) \rangle$ [see Eq. (3)] and of the associated current $\langle \mathcal{J}_j(t) \rangle$, with

$$\mathcal{J}_j = Jh_z(\sigma_{j-1}^x\sigma_j^y - \sigma_j^y\sigma_{j+1}^x), \quad (4)$$

for various values of $h_{x,z}$. The results of the simulations are illustrated in Fig. 1 only up to times $t = 50J^{-1}$, as no qualitative differences are observed up to t_M . In both the “strong” ($h_x \gg h_z$) and “weak” ($h_x \lesssim h_z$) confinement regime, energy transfer between the two halves of the chain is suppressed even at late times. As shown in Fig. 1, the main dynamical effect of switching on h_z is given by pronounced oscillations of the profiles around the position $j = L/2$ of the junction, with characteristic emergent amplitudes and frequencies

which depend on the values of the fields. In particular, the energy current density is zero everywhere apart around the junction, where it oscillates between positive values (aligned with the energy gradient) and negative values (against the energy gradient). We emphasize that, within our protocol, an increase in the energy gradient between the two halves, caused by a stronger h_x , does not result in the activation of transport: On the contrary, it turns out that the oscillations at the junction acquire an even smaller amplitude (see Fig. 1 from top to bottom).

Effective dynamics. The oscillations of the profiles shown in Fig. 1 may be interpreted as the quantum motion of the isolated kink initially localized at the junction, triggered by the transverse field $h_z \neq 0$. In fact, the kinetic energy associated with this motion has a finite bandwidth $\sim h_z$ on the lattice, and therefore, because of energy conservation, the kink quasiparticle can travel, in the linear confining potential $V(l) \sim -h_x l$, at most a distance $l_{\text{conf}} \sim h_z/h_x$ (confinement length scale), before bouncing back and oscillating. This phenomenon is analogous to the Wannier-Stark localization of electrons in a one-dimensional crystal subject to a constant electric field [75,76].

In order to rationalize the above intuition and make a quantitative treatment of the evolution of the profiles, we propose a simple analytical approach based on dressing the meson quasiparticles perturbatively in the transverse field $h_z \ll J$, with arbitrary h_x . (This regime differs from the one $h_x \ll J$, $h_z < J$, of validity of the semiclassical technique of Ref. [70].) The approximation consists in neglecting the creation of new quasiparticles, which, in our setup, only affect the quantum fluctuations in the two homogeneous bulks away from the junction, as recognized in Refs. [54,70]. In fact, we show that the dynamics at the junction is very well captured within this scheme up to moderate values of h_z .

In the spirit of an effective quasiparticle description of mesons [77], we map the motion of the isolated kink onto the problem of a *single quantum particle* hopping on a one-dimensional lattice, by projecting the many-body Hilbert space onto the single-kink linear subspace [78]. As the numerical results indicate (see Fig. 1), for $h_z \ll J$ and arbitrary h_x ,¹ the dynamics can be approximated within this subspace, spanned by the states $\{|n\rangle\}$ with a single domain wall located between sites n and $n+1$, with $n = 1, 2, \dots, L-1$. The corresponding unperturbed energy eigenvalues are $E_n = 2J + 2h_x(L-n) + E_{\text{GS}}$ where $E_{\text{GS}} = -J(L-1) - h_x L$ is the ground state energy. The resulting matrix elements $\langle n | H(h_z, h_x) | m \rangle$ of the Hamiltonian (1) read $E_{\text{GS}} \delta_{n,m} + (H^{\text{eff}})_{nm}$, with

$$(H^{\text{eff}})_{nm} = [2J + 2(L-n)h_x] \delta_{n,m} - h_z(\delta_{n,m+1} + \delta_{n,m-1}). \quad (5)$$

¹Note, however, that resonances occur at particular values of h_x , commensurate with $2J$. Correspondingly, it costs no energy to break a single meson into multiple mesons by flipping individual spins. These transitions cause quantitative but not qualitative modifications to the evolution of the energy profile, which are not captured by the single-kink subspace projection discussed here. Evidence of this aspect can be found in the Supplemental Material.

We note that the off-diagonal perturbation produces an effective hopping amplitude for the kink quasiparticle. Accordingly, the effective Hamiltonian H^{eff} describes the dynamics in terms of a single-particle hopping in a one-dimensional lattice in the presence of a linear potential, where the state of the particle is described by a vector $\{\psi_n\}$ with $n = 1, 2, \dots, L-1$. The absolute value squared of the n th component of the wave function $\psi_n(t)$ is equal to the probability that the particle is at site n at time t . Within this picture, the initial state in Eq. (2) maps to $\psi_n(0) = \delta_{n,L/2}$, corresponding to a particle completely localized at the junction between the two chains. Similarly, the magnetization $\langle \sigma_j^x(t) \rangle$ at site j and time t can be expressed [78] within this single-particle picture as

$$m_j(t) \equiv 1 - 2 \sum_{n=1}^{j-1} |\psi_n(t)|^2, \quad (6)$$

where $\psi_n(t) = \sum_m [\exp(-iH^{\text{eff}}t)]_{nm} \psi_m(0)$ is the time evolved state within the projected space.

In order to test the accuracy of our approximation, we compare the dynamics obtained from the above effective single-particle problem with the exact dynamics generated by H [see Eq. (1)] in the full many-body Hilbert space, starting from the domain-wall initial state $|\Psi_0\rangle$ of Eq. (2) as obtained via both exact diagonalization (ED) and TEBD techniques.² The comparison between $m_{L/2}(t)$ and $\langle \sigma_{L/2}^x(t) \rangle$ is shown in Fig. 2. In particular, we observe that the agreement is fairly good up to moderate values of the transverse field $h_z \lesssim 0.4J$.

Similarly, the relevant nonequilibrium profiles of the energy and energy current densities can be studied within the above effective single-particle description. This is achieved by projecting the energy density \mathcal{H}_j at site j in Eq. (3) onto the single-kink subspace,

$$(\mathcal{H}_j^{\text{eff}})_{nm} = \frac{1}{2}[J(2\delta_{j,n} - 1) - h_x \text{sgn}(n-j)] \delta_{n,m} - \frac{h_z}{2}(\delta_{j,m+1} + \delta_{j+1,m+1}) \delta_{n,m+1} + (m \leftrightarrow n), \quad (7)$$

where the sign function $\text{sgn}(x)$ equals 1 for $x > 0$, -1 for $x < 0$, and 0 for $x = 0$. From the continuity equation

$$\frac{d\mathcal{H}_j^{\text{eff}}}{dt} = i[H^{\text{eff}}, \mathcal{H}_j^{\text{eff}}] = \mathcal{J}_j^{\text{eff}} - \mathcal{J}_{j+1}^{\text{eff}}, \quad (8)$$

we can infer the corresponding effective expression for the energy current density operator \mathcal{J}_j at site j , i.e.,

$$(\mathcal{J}_j^{\text{eff}})_{nm} = 2iJh_z \delta_{n,m+1} \delta_{m,j-1} - \frac{i}{2}h_z^2 \delta_{m,j-2} \delta_{n,m+2} - \frac{i}{2}h_z^2 \delta_{m,j-1} \delta_{n,m+2} - (m \leftrightarrow n). \quad (9)$$

The time-dependent expectation value of the energy density at site j within this single-particle picture can therefore be

²In this case, the simulations based on exact diagonalization of the Hamiltonian can be pushed until sufficiently late times because finite-size effects such as revivals are suppressed, due to the fact that excitations are confined [54].

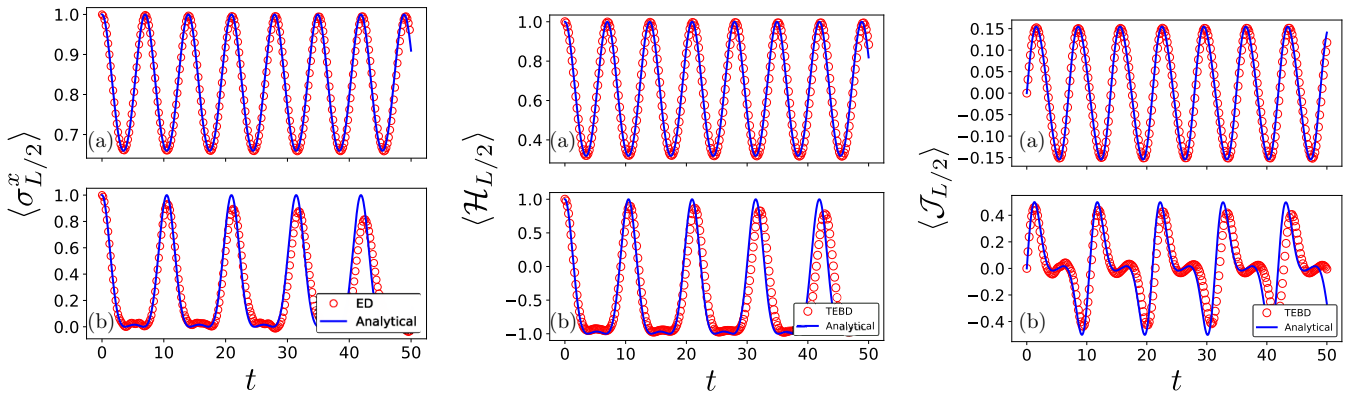


FIG. 2. Comparison between the numerical results $\langle \sigma_{L/2}^x(t) \rangle$, $\langle \mathcal{H}_{L/2}(t) \rangle$, $\langle \mathcal{J}_{L/2}(t) \rangle$ (symbols), and the analytical predictions $m_{L/2}(t)$, $e_{L/2}(t)$, $j_{L/2}(t)$ (solid lines) for the magnetization (left panel), energy density (central panel), and energy density current (right panel), respectively, at the junction $j = L/2$, as obtained from ED (with $L = 16$) or TEBD (with $L = 50$ or 100), and from the effective single-particle model, respectively. These curves refer to $h_x = 0.45$, $h_z = 0.2$ (top row), and $h_x = 0.3$, $h_z = 0.4$ (bottom row). (Units are fixed such that $J = 1$.) Note that discrepancies between symbols and solid lines appear as time increases, due to the neglected multikink processes. The associated timescale, however, increases upon decreasing h_z .

written as

$$e_j(t) \equiv \sum_{n,m} \psi_n^*(t) (\mathcal{H}_j^{\text{eff}})_{nm} \psi_m(t), \quad (10)$$

with an analogous expression for the current $j_j(t)$ in terms of $\mathcal{J}_j^{\text{eff}}$. In Fig. 2 we compare the time evolution of $e_{L/2}(t)$ and $j_{L/2}(t)$ with the corresponding exact quantities $\langle \mathcal{H}_{L/2}(t) \rangle$ and $\langle \mathcal{J}_{L/2}(t) \rangle$ as obtained from the TEBD simulations. [One can show that the spectrum of the effective Hamiltonian (5) consists of multiples of $2h_x$, which results in exactly periodic behavior of the blue lines in Fig. 2.] It is remarkable that, in spite of the simplicity of this approach, the agreement is excellent for small values $h_z = 0.2J$ of the transverse field, whereas for larger values $h_z = 0.4J$, small quantitative discrepancies appear, still retaining a fairly good qualitative agreement.

Conclusions. In a homogeneous quench, the confinement of excitations has been recently shown to hinder the spreading of correlations in the quantum Ising chain (1) with both transverse and longitudinal magnetic fields [54]. (Anomalous nonequilibrium evolution had already been reported in the same model, but within a different regime of parameters, in Refs. [77,79].) In this Rapid Communication, we have shown that this phenomenon has significant consequences even in inhomogeneous setups, as it can lead to suppression of energy transport. This lack of transport in the presence of an initial gradient actually mirrors the fact that the spatial inhomogeneity in the longitudinal magnetization persists at long times, meaning that the system fails to locally relax to the thermal ensemble up to the largest accessible and explored times, $t_M = 10^3 J^{-1}$, which are longer than those currently accessible in experiments.

We emphasize that in the problem discussed here the specific choice of the class of inhomogeneous initial states plays an important role. As we have shown, the nonequilibrium dynamics is accurately captured by the boundary Bloch oscillations of a single macroscopically large “meson.” Based

on extensive numerical work, it has been recently suggested in Ref. [80] that the Hamiltonian (1) is characterized by a pattern of atypical energy eigenstates with nonthermal features carrying over to the thermodynamic limit, which violate the eigenstate thermalization hypothesis [81]. In this light, our results may represent a dynamical manifestation of this phenomenon. In particular, if the initial states have significant overlap with those “single-meson” nonthermal eigenstates, the initial inhomogeneity would persist to *infinite* time. However, we argue that more general initial states, with magnetic domains separated by distances much larger than the confinement length scale, would also retain their inhomogeneity for a correspondingly long time.

The phenomenon reported here may be interpreted as a dramatic slowdown or suppression of “string breaking” in one-dimensional quantum models with confinement of excitations. As such, we expect it to occur rather generically in this context, e.g., in XXZ spin chains [55–58], one-dimensional extended Bose-Hubbard models [60,82], spin-1 quantum chains [61,83], and systems with long-range interactions [59,84], as well as lattice models of quantum electrodynamics [64]. Similarly, we observe that recent works have reported the occurrence of localization phenomena—and thereby of suppression of information spreading—within the context of lattice gauge theories, where confinement of elementary excitations naturally arises as well [62–64,82,85–87]. In future work we plan to investigate the very origin of this seemingly ubiquitous phenomenon, as well as to address the important problem of estimating the relaxation timescales.

Acknowledgments. We acknowledge useful discussions with P. Calabrese, G. B. Mbeng, J. Moore, G. Pagano, N. Robinson, and S. B. Rutkevich. We thank G. Giudici for technical help with the numerical codes. The work of M.C. was supported by the European Union’s Horizon 2020 research and innovation programme under the Marie Skłodowska-Curie Grant Agreement No. 701221.

- [1] P. Calabrese, F. H. L. Essler, and G. Mussardo, *J. Stat. Mech.* (2016) 064001.
- [2] J. Eisert, M. Friesdorf, and C. Gogolin, *Nat. Phys.* **11**, 124 (2015).
- [3] A. Polkovnikov, K. Sengupta, A. Silva, and M. Vengalattore, *Rev. Mod. Phys.* **83**, 863 (2011).
- [4] M. Greiner, O. Mandel, T. W. Hänsch, and I. Bloch, *Nature (London)* **419**, 51 (2002).
- [5] T. Kinoshita, T. Wenger, and D. S. Weiss, *Nature (London)* **440**, 900 (2006).
- [6] S. Hofferberth, I. Lesanovsky, B. Fischer, T. Schumm, and J. Schmiedmayer, *Nature (London)* **449**, 324 (2007).
- [7] L. Hackermüller, U. Schneider, M. Moreno-Cardoner, T. Kitagawa, T. Best, S. Will, E. Demler, E. Altman, I. Bloch, and B. Paredes, *Science* **327**, 1621 (2010).
- [8] S. Trotzky, Y.-A. Chen, A. Flesch, I. P. McCulloch, U. Schollwöck, J. Eisert, and I. Bloch, *Nat. Phys.* **8**, 325 (2012).
- [9] M. Gring, M. Kuhnert, T. Langen, T. Kitagawa, B. Rauer, M. Schreitl, I. Mazets, D. Adu Smith, E. Demler, and J. Schmiedmayer, *Science* **337**, 1318 (2012).
- [10] M. Cheneau, P. Barmettler, D. Poletti, M. Endres, P. Schauss, T. Fukuhara, C. Gross, I. Bloch, C. Kollath, and S. Kuhr, *Nature (London)* **481**, 484 (2012).
- [11] T. Langen, R. Geiger, M. Kuhnert, B. Rauer, and J. Schmiedmayer, *Nat. Phys.* **9**, 640 (2013).
- [12] F. Meinert, M. J. Mark, E. Kirilov, K. Lauber, P. Weinmann, A. J. Daley, and H.-C. Nägerl, *Phys. Rev. Lett.* **111**, 053003 (2013).
- [13] J. P. Ronzheimer, M. Schreiber, S. Braun, S. S. Hodgman, S. Langer, I. P. McCulloch, F. Heidrich-Meisner, I. Bloch, and U. Schneider, *Phys. Rev. Lett.* **110**, 205301 (2013).
- [14] L. Vidmar, J. P. Ronzheimer, M. Schreiber, S. Braun, S. S. Hodgman, S. Langer, F. Heidrich-Meisner, I. Bloch, and U. Schneider, *Phys. Rev. Lett.* **115**, 175301 (2015).
- [15] I. Bloch, *Nat. Phys.* **1**, 23 (2005).
- [16] B. Paredes, A. Widera, V. Murg, O. Mandel, S. Fölling, I. Cirac, G. V. Shlyapnikov, T. W. Hänsch, and I. Bloch, *Nature (London)* **429**, 277 (2004).
- [17] R. Jördens, N. Strohmaier, K. Günter, H. Moritz, and T. Esslinger, *Nature (London)* **455**, 204 (2008).
- [18] S. Palzer, C. Zipkes, C. Sias, and M. Köhl, *Phys. Rev. Lett.* **103**, 150601 (2009).
- [19] C. C. Chien, S. Peotta, and M. Di Ventra, *Nat. Phys.* **11**, 998 (2015).
- [20] S. Jezouin, F. D. Parmentier, A. Anthore, U. Gennser, A. Cavanna, Y. Jin, and F. Pierre, *Science* **342**, 601 (2013).
- [21] S. Datta, *Electronic Transport in Mesoscopic Systems* (Cambridge University Press, Cambridge, U.K., 1995).
- [22] E. Akkermans and G. Montambaux, *Mesoscopic Physics of Electrons and Photons* (Cambridge University Press, Cambridge, U.K., 2007).
- [23] P. Calabrese and J. Cardy, *Phys. Rev. Lett.* **96**, 136801 (2006).
- [24] P. Calabrese and J. Cardy, *J. Stat. Mech.* (2007) P06008.
- [25] F. Iglói, and H. Rieger, *Phys. Rev. Lett.* **106**, 035701 (2011).
- [26] H. Rieger, and F. Iglói, *Phys. Rev. B* **84**, 165117 (2011).
- [27] F. H. L. Essler and M. Fagotti, *J. Stat. Mech.* (2016) 064002.
- [28] D. Bernard and B. Doyon, *J. Stat. Mech.* (2016) 064005.
- [29] A. De Luca, J. Viti, D. Bernard, and B. Doyon, *Phys. Rev. B* **88**, 134301 (2013).
- [30] T. Antal, Z. Rácz, A. Rákos, and G. M. Schütz, *Phys. Rev. E* **59**, 4912 (1999).
- [31] J. Viti, J. M. Stephán, J. Dubail, and M. Haque, *Europhys. Lett.* **115**, 40011 (2016).
- [32] A. Biella, A. De Luca, J. Viti, D. Rossini, L. Mazza, and R. Fazio, *Phys. Rev. B* **93**, 205121 (2016).
- [33] M. Collura and D. Karevski, *Phys. Rev. B* **89**, 214308 (2014).
- [34] G. Peretto and A. Gambassi, *Phys. Rev. E* **96**, 012138 (2017).
- [35] M. Kormos, *Sci. Post Phys.* **3**, 020 (2017).
- [36] V. Eisler, F. Maislinger, and H. G. Evertz, *SciPost Phys.* **1**, 014 (2016).
- [37] B. Bertini, M. Collura, J. De Nardis, and M. Fagotti, *Phys. Rev. Lett.* **117**, 207201 (2016).
- [38] O. A. Castro-Alvaredo, B. Doyon, and T. Yoshimura, *Phys. Rev. X* **6**, 041065 (2016).
- [39] P. W. Anderson, *Phys. Rev.* **109**, 1492 (1958).
- [40] D. M. Basko, I. L. Aleiner, and B. L. Altshuler, *Ann. Phys.* **321**, 1126 (2006).
- [41] V. Oganesyan and D. A. Huse, *Phys. Rev. B* **75**, 155111 (2007).
- [42] D. A. Huse, R. Nandkishore, and V. Oganesyan, *Phys. Rev. B* **90**, 174202 (2014).
- [43] J. Z. Imbrie, V. Ros, and A. Scardicchio, *Ann. Phys. (Berlin)* **529**, 1600278 (2017).
- [44] M. Serbyn, Z. Papić, and D. A. Abanin, *Phys. Rev. X* **5**, 041047 (2015).
- [45] V. K. Varma, A. Leroze, F. Pietracaprina, J. Goold, and A. Scardicchio, *J. Stat. Mech.* (2017) 053101.
- [46] M. Žnidarič, A. Scardicchio, and V. K. Varma, *Phys. Rev. Lett.* **117**, 040601 (2016).
- [47] R. Vasseur and J. E. Moore, *J. Stat. Mech.* (2016) 064010.
- [48] M. Žnidarič, T. Prosen, and P. Prelovšek, *Phys. Rev. B* **77**, 064426 (2008).
- [49] J. H. Bardarson, F. Pollmann, and J. E. Moore, *Phys. Rev. Lett.* **109**, 017202 (2012).
- [50] N. Y. Yao, C. R. Laumann, J. I. Cirac, M. D. Lukin, and J. E. Moore, *Phys. Rev. Lett.* **117**, 240601 (2016).
- [51] S. Lorenzo, T. Apollaro, G. M. Palma, R. Nandkishore, A. Silva, and J. Marino, *Phys. Rev. B* **98**, 054302 (2018).
- [52] B. M. McCoy and T. T. Wu, *Phys. Rev. D* **18**, 1259 (1978).
- [53] R. Shankar and G. Murthy, *Phys. Rev. B* **72**, 224414 (2005).
- [54] M. Kormos, M. Collura, G. Takács, and P. Calabrese, *Nat. Phys.* **13**, 246 (2017).
- [55] Z. Cai, C. Wu, and U. Schollwöck, *Phys. Rev. B* **85**, 075102 (2012).
- [56] Z. Wang, M. Schmidt, A. K. Bera, A. T. M. N. Islam, B. Lake, A. Loidl, and J. Deisenhofer, *Phys. Rev. B* **91**, 140404(R) (2015).
- [57] A. K. Bera, B. Lake, F. H. L. Essler, L. Vanderstraeten, C. Hubig, U. Schollwöck, A. T. M. N. Islam, A. Schneidewind, and D. L. Quintero-Castro, *Phys. Rev. B* **96**, 054423 (2017).
- [58] S. B. Rutkevich, *Europhys. Lett.* **121**, 37001 (2018).
- [59] F. Liu, R. Lundgren, P. Titum, G. Pagano, J. Zhang, C. Monroe, and A. V. Gorshkov, *Phys. Rev. Lett.* **122**, 150601 (2019).
- [60] Y. Kuno, S. Sakane, K. Kasamatsu, I. Ichinose, and T. Matsui, *Phys. Rev. D* **95**, 094507 (2017).
- [61] T. Suzuki and S.-i. Suga, *Phys. Rev. B* **98**, 180406(R) (2018).
- [62] T. Pichler, M. Dalmonte, E. Rico, P. Zoller, and S. Montangero, *Phys. Rev. X* **6**, 011023 (2016).
- [63] P. Sala, T. Shi, S. Kühn, M. C. Banuls, E. Demler, and J. I. Cirac, *Phys. Rev. D* **98**, 034505 (2018).

- [64] F. M. Surace, P. P. Mazza, G. Giudici, A. Lerose, A. Gambassi, and M. Dalmonte, [arXiv:1902.09551](https://arxiv.org/abs/1902.09551).
- [65] E. Lieb, T. Schultz, and D. Mattis, *Ann. Phys.* **16**, 407 (1961).
- [66] S. A. Pikin and V. M. Tsukernik, *Zh. Eksp. Teor. Fiz.* **50**, 1377 (1966) [*Sov. Phys. JETP* **23**, 914 (1966)].
- [67] P. Pfeuty, *Ann. Phys.* **57**, 79 (1970).
- [68] G. Delfino, P. Grinza, and G. Mussardo, *Nucl. Phys. B* **737**, 291 (2006).
- [69] P. Fonseca and A. Zamolodchikov, [arXiv:hep-th/0612304](https://arxiv.org/abs/hep-th/0612304).
- [70] S. B. Rutkevich, *J. Stat. Phys.* **131**, 917 (2008).
- [71] R. J. Rubin and W. L. Greer, *J. Math. Phys.* **12**, 1686 (1971).
- [72] H. Spohn and J. L. Lebowitz, *Commun. Math. Phys.* **54**, 97 (1977).
- [73] S. B. Rutkevich, *Phys. Rev. B* **60**, 14525 (1999).
- [74] G. Vidal, *Phys. Rev. Lett.* **98**, 070201 (2007).
- [75] G. H. Wannier, *Elements of Solid State Theory* (Praeger, Santa Barbara, CA, 1970).
- [76] H. Fukuyama, R. A. Bari, and H. C. Fogedby, *Phys. Rev. B* **8**, 5579 (1973).
- [77] C.-J. Lin and O. I. Motrunich, *Phys. Rev. A* **95**, 023621 (2017).
- [78] See Supplemental Material at <http://link.aps.org/supplemental/10.1103/PhysRevB.99.180302> for technical details concerning the calculation of the effective quantities.
- [79] M. C. Banuls, J. I. Cirac, and M. B. Hastings, *Phys. Rev. Lett.* **106**, 050405 (2011).
- [80] A. J. A. James, R. M. Konik, and N. J. Robinson, *Phys. Rev. Lett.* **122**, 130603 (2019).
- [81] L. D'Alessio, Y. Kafri, A. Polkovnikov, and M. Rigol, *Adv. Phys.* **65**, 239 (2016).
- [82] J. Park, Y. Kuno, and I. Ichinose, [arXiv:1903.07297](https://arxiv.org/abs/1903.07297).
- [83] T. Suzuki and S. Suga, *J. Phys. Soc. Jpn.* **88**, 053702 (2019).
- [84] A. Lerose, B. Žunkovič, A. Silva, and A. Gambassi, *Phys. Rev. B* **99**, 121112(R) (2019).
- [85] R. M. Nandkishore and S. L. Sondhi, *Phys. Rev. X* **7**, 041021 (2017).
- [86] A. Smith, J. Knolle, D. L. Kovrizhin, and R. Moessner, *Phys. Rev. Lett.* **118**, 266601 (2017).
- [87] M. Brenes, M. Dalmonte, M. Heyl, and A. Scardicchio, *Phys. Rev. Lett.* **120**, 030601 (2018).